J. Fluid Mech. (2000), *vol.* 403, *pp.* 23–36. Printed in the United Kingdom

LES computations and comparison with Kolmogorov theory for two-point pressure–velocity correlations and structure functions for globally anisotropic turbulence

By K. ALVELIUS AND A. V. JOHANSSON

Department of Mechanics, KTH, SE-100 44 Stockholm, Sweden

(Received 6 November 1998 and in revised form 31 August 1999)

A new extension of the Kolmogorov theory, for the two-point pressure–velocity correlation, is studied by LES of homogeneous turbulence with a large inertial subrange in order to capture the high Reynolds number nonlinear dynamics of the flow. Simulations of both decaying and forced anisotropic homogeneous turbulence were performed. The forcing allows the study of higher Reynolds numbers for the same number of modes compared with simulations of decaying turbulence. The forced simulations give statistically stationary turbulence, with a substantial inertial subrange, well suited to test the Kolmogorov theory for turbulence that is locally isotropic but has significant anisotropy of the total energy distribution. This has been investigated in the recent theoretical studies of Lindborg (1996) and Hill (1997) where the role of the pressure terms was given particular attention. On the surface the two somewhat different approaches taken in these two studies may seem to lead to contradictory conclusions, but are here reconciled and (numerically) shown to yield an interesting extension of the traditional Kolmogorov theory. The results from the simulations indeed show that the two-point pressure–velocity correlation closely adheres to the predicted linear relation in the inertial subrange where also the pressure-related term in the general Kolmogorov equation is shown to vanish. Also, second- and third-order structure functions are shown to exhibit the expected dependences on separation.

1. Introduction

In a typical turbulent flow there is production of turbulence kinetic energy at large scales. This energy is on average transported to smaller scales where it is dissipated. If there is a large separation between the energy-producing scales and the dissipative scales we have a range, the inertial subrange, where the dynamics of the turbulence is unaffected by the mechanisms of production and dissipation. In his classical papers Kolmogorov (1941*a*,*b*) derived the now famous inertial-range laws. As a starting point, and a central tool in the analysis, he used correlations of velocity differences $\delta \boldsymbol{u} = \boldsymbol{u}' - \boldsymbol{u}$ between two points, separated by a distance $\boldsymbol{r}$, to analyse the turbulence structures at small scales. These correlations

$$B^{(n)}_{ij..k} = \langle \delta u_i \delta u_j \cdots \delta u_k \rangle \tag{1.1}$$

are usually referred to as nth-order structure functions, and have been used extensively in the search for an improved understanding of turbulence dynamics, see e.g. Frisch (1995). Here $\langle \cdots \rangle$ denotes ensemble averaging over an infinite number of realizations.

Under the assumption of statistical stationarity and global isotropy Kolmogorov (1941*a*) derived the equation

$$B_{lll} = -\tfrac{4}{5}\epsilon r + 6\nu \frac{\partial B_{ll}}{\partial r}, \tag{1.2}$$

relating the third- and second-order structure functions B_{lll} and B_{ll}, where the index l denotes a velocity component in the same direction as $\boldsymbol{r}$ and ϵ is the dissipation rate of the kinetic energy, $K \equiv \langle u_i u_i \rangle / 2$. In the present paper the index t will denote a velocity component orthogonal to $\boldsymbol{r}$ (no summation over repeated indices l and t). If the Reynolds number is high enough there is a range of separations r where the viscous term in (1.2) can be neglected compared to the others and the well-known four-fifths law for the third-order structure function B_{lll} is recovered.

The derivation of (1.2) has been the subject of much attention recently (Lindborg 1996 and Hill 1997) in order to relax the condition of global isotropy to only require local isotropy. In the work of Monin & Yaglom (1975) an analysis is given from which they conclude that the pressure terms, including the two-point pressure–velocity correlation

$$P_l(r) = \frac{1}{\rho}\left(\langle p' u_l \rangle - \langle p u_l' \rangle\right), \tag{1.3}$$

vanish in the inertial range. Lindborg (1996) showed that they in fact used the assumption of global isotropy instead of local isotropy in their derivation. He further showed that in order to reduce the general Kolmogorov equations, under the assumption of global homogeneity, to the equation (1.2) the pressure related terms need to balance each other. This gives a linear relation for the two-point pressure–velocity correlation in the inertial range

$$P_l(r) = -\Pi_{ll} r, \tag{1.4}$$

where $\Pi_{ij} \equiv 2\langle p s_{ij} \rangle / \rho$ is the pressure–strain rate tensor and $s_{ij} \equiv 0.5(u_{i,j} + u_{j,i})$ is the fluctuating part of the strain tensor. The four-fifths law together with the additional relationship (1.4) was, hence, shown to be valid in globally homogeneous and locally isotropic turbulence. Hill (1997) derived the Kolmogorov equation (1.2) under the weaker assumption of only requiring local homogeneity and local isotropy. In his derivation he showed that the pressure term

$$T_{ij}(\boldsymbol{r}) = \frac{1}{\rho}\left(\left\langle \left(u_i - u_i'\right)\left(\frac{\partial p}{\partial x_j} - \frac{\partial p'}{\partial x_j'}\right)\right\rangle + \left\langle \left(u_j - u_j'\right)\left(\frac{\partial p}{\partial x_i} - \frac{\partial p'}{\partial x_i'}\right)\right\rangle\right) \tag{1.5}$$

is zero in the inertial range. Yaglom (1998) expressed a suspicion that the results of Hill may contradict those of Lindborg. However, Lindborg (1999*b*) showed that the relation (1.4) can be derived from the condition $T_{ij} = 0$ in locally homogeneous turbulence. The derivation of the relation $T_{ij} = 0$ only requires local homogeneity, local isotropy and incompressibility. It is hence valid for any scalar field p and divergence-free vector field u_i satisfying local homogeneity and local isotropy.

The pressure–strain rate has the role of redistributing energy from velocity components with a high energy content to those with less. The modelling of Π_{ij} is a key issue in turbulence closures based on the Reynolds stress transport equations. To a large extent it determines the return-to-isotropy process in freely decaying turbulence,

but also has a dominating role in the intercomponent energy distribution in strained flows and turbulence subjected to rotation.

For separations close to the dissipative Kolmogorov scale $\eta = (\nu^3/\epsilon)^{1/4}$ the behaviour of the two-point correlations is obtained from Taylor expansion, from which it is readily found that the structure functions vary as $B^{(n)} \sim r^n$ as $r \to 0$. We may note that this is a behaviour different from that in the inertial range. However, the correlation P_l retains its linear (inertial range) behaviour all the way to zero separation. The theory of Lindborg (1996) in fact shows that the second-order term in the Taylor expansion for P_l is small even for inertial-range separations.

It is difficult to measure the pressure fluctuations accurately in an experiment. In a direct numerical simulation (DNS) the pressure fluctuations can be computed with high accuracy. However, DNS are still limited to relatively low Reynolds numbers. LES has the potential to give a large $k^{-5/3}$ range for the energy spectrum, $E(k)$, and should be well suited for this investigation. For such an LES the number of grid points needs to be large in the inertial subrange in order to investigate the possibility of a linear behaviour of P_l and B_{lll} and to verify that $T_{ij} = 0$.

For the purpose of numerical investigation it is important to note that the Kolmogorov theory is valid at lower Reynolds number for statistically stationary turbulence as compared to decaying turbulence as has recently been discussed and illustrated numerically by Lindborg (1999*a* and Alvelius (1999). This can be attributed to the increased extent of the equilibrium range of the spectrum, where the rate of change of the spectral energy density can be neglected in the dynamic equation. In the general Kolmogorov equation of non-stationary flows there is an extra time derivative term of B_{ll} which in addition to the viscous term also needs to be small. This condition is trivially satisfied in the stationary case, whereas it is only satisfied for sufficiently small separations in the two-point correlations of decaying turbulence.

The main aim of the present study is to numerically test the theory (1.4) of Lindborg (1996) for the two-point pressure–velocity correlation and to verify the results from the classical Kolmogorov equation in globally anisotropic turbulence. Also the conclusion of Hill (1997) that $T_{ij} = 0$ in the inertial range is tested with the aid of the present numerical simulation. For the reasons given above both decaying and forced homogeneous simulations have been performed, where a better agreement with theory is expected for the forced simulations.

2. The LES

The governing equations in LES are the filtered Navier–Stokes (NS) and continuity equations for incompressible flow

$$\frac{\partial \bar{u}_i}{\partial t} + \bar{u}_j \frac{\partial \bar{u}_i}{\partial x_j} = -\frac{1}{\rho}\frac{\partial \bar{p}}{\partial x_i} + \nu \frac{\partial^2 \bar{u}_i}{\partial x_j \partial x_j} - \frac{\partial \tau_{ij}}{\partial x_j} + \bar{f}_i, \tag{2.1}$$

$$\frac{\partial \bar{u}_k}{\partial x_k} = 0, \tag{2.2}$$

where an overline denotes a filtered quantity and $\tau_{ij} = \overline{u_i u_j} - \bar{u}_i \bar{u}_j$ is the subgrid-scale (SGS) stress tensor which has to be modelled (the ensemble-averaged mean flow is here zero); $\bar{f}_i$ is a random volume force which is zero in the decaying turbulence simulations. The modelled equations are solved in a box with periodic boundary conditions. In the case of homogeneous turbulence the main task of the SGS model

is to provide the correct energy transfer from the resolved scales to the subgrid scales. Since the LES only solves for the filtered velocity field the small-scale behaviour as $r \to 0$ cannot be captured.

In the present simulations the flow is relatively well resolved in order to reduce the importance of the SGS stress model. The results of Lindborg (1996) state that the main contribution to the pressure is from the large scales of the flow, and the direct influence from the SGS stress model is small. Also, the pressure spectrum decays as $k^{-7/3}$ in the inertial subrange, which yields a small contribution from the smaller scales. This suggest that LES should be well suited for predictions of quantities involving the pressure. Alvelius, Hallbäck & Johansson (1999) have shown that indeed the contributions to e.g. the pressure–strain rate are dominated by the large scales and that the contribution from the subgrid scales is negligible in an LES with the Smagorinsky model.

2.1. *The forcing*

The random forcing method of Alvelius (1999) was used in the present simulations to generate statistically stationary anisotropic turbulence states. The random volume force is divergence free and implemented in Fourier space at low wavenumbers. It introduces energy into the flow at large scales, which is, on average, transported through the action of the energy cascade to smaller scales where it is dissipated. The force is completely random in time and over the wavenumbers where it is active. The randomness makes the force neutral in the sense that it does not introduce or enhance any particular structure or timescale of the turbulence. The energy spectrum of the forcing is Gaussian with the peak at wavenumber k_f. Since the force is completely random in time the contribution from the velocity–force correlation to the power input is zero on average, and all the net power input comes from the force–force correlation which is controllable. The total amount of power and its distribution among the velocity components is determined *a priori*. It is hence possible to generate statistically stationary anisotropic states by the forcing.

2.2. *The SGS stress tensor*

Both the Smagorinsky (1963) model and the spectral (Chollet 1984) model are used to describe the SGS stress tensor. These have proved successful in various flow cases, e.g. isotropic turbulence for the spectral model (Chasnov 1991) and plane channel flow for the Smagorinsky model (Piomelli 1994). The anisotropy of the energy distribution in the present simulations should not cause any problems for the spectral model since there is a large range of scales between the large anisotropic scales and the small isotropic scales where the model acts.

The spectral Chollet (1984) model is implemented in spectral space as

$$i k_k \hat{\tau}_{ik} = \nu_T(k) k^2 \hat{\tilde{u}}_i, \tag{2.3}$$

$$\nu_T(k) = Ko^{-3/2} \left[0.441 + 15.2 \exp\left(\frac{-3.03 k_c}{k} \right) \right] \sqrt{\frac{E(k_c)}{k_c}}, \tag{2.4}$$

where a hat denotes the Fourier transform, $\boldsymbol{k}$ is the wavenumber vector and k_c is the cut-off wavenumber. The parameter Ko should be adjusted so that it equals the Kolmogorov constant related to the kinetic energy spectrum. The derivation of the model suggests that it should be used together with a 'spherical' spectral cut-off filter

$$\widehat{G}(k) = \begin{cases} 1 & \text{if } |k| \leqslant k_c, \\ 0 & \text{otherwise.} \end{cases} \tag{2.5}$$

The contribution from the SGS stresses to the pressure in the Poisson equation enters in Fourier space as $k_i k_j \hat{\tau}_{ij}$. This term is however zero for the spectral model which implies that the SGS stress model does not directly influence the pressure which, however, the real SGS stress tensor does. The effect of the model only enters indirectly through the resolved velocity field.

The spectral model, which was derived for a $k^{-5/3}$ inertial energy spectrum at the cut-off wavenumber, k_c, has been modified to handle flows with an energy spectrum slope steeper than $k^{-5/3}$ at k_c (Métais & Lesieur 1992). It has also been extended to a physical space implementation (Métais & Lesieur 1992), which allows it to handle non-homogeneous flows. Since we only consider homogeneous flows with inertial subrange behaviour, none of these modifications are needed for the present simulations.

The Smagorinsky (1963) model for the SGS stress tensor reads

$$\tau_{ij} = \tfrac{1}{3}\tau_{kk}\delta_{ij} - 2\nu_T \bar{s}_{ij}, \tag{2.6}$$

$$\nu_T = (C_s L)^2 (2\bar{s}_{pq}\bar{s}_{pq})^{1/2}, \tag{2.7}$$

where $\bar{s}_{ij} = (\bar{u}_{i,j} + \bar{u}_{j,i})/2$, L is a filter width and C_s is the Smagorinsky constant. The Smagorinsky model is implemented together with a 'cubic' spectral cut-off filter, which in spectral space reads

$$\widehat{G}(\boldsymbol{k}) = \begin{cases} 1 & \text{if } |k_i| \leqslant k_c^i, \quad i = 1,2,3, \\ 0 & \text{otherwise,} \end{cases} \tag{2.8}$$

where k_c^i are the cut-off wavenumbers in the three directions ($i = 1, 2, 3$). We follow the approach of Deardorff (1970) and base the filter width on the grid volume $L \equiv \pi/(k_c^1 k_c^2 k_c^3)^{1/3}$, which is a reasonable choice for moderately strained meshes. The trace τ_{kk} is not modelled and therefore treated together with the pressure.

The original Smagorinsky model was extended through the dynamical approach (Germano *et al.* 1991), in which the Smagorinsky constant is determined locally by the flow, to perform better in non-homogeneous flows. In particular this method reduces the constant close to solid walls which eliminates the need for wall damping functions. This constant is usually averaged over homogeneous directions. In the present flow case, with three homogeneous directions, this would yield a Smagorinsky constant that depends on time only. In the statistically stationary flow case the value of the constant can be determined empirically so that a $k^{-5/3}$ kinetic energy spectrum is obtained, hence eliminating the need for dynamic determination of the model parameter.

Another extension is the mixed model by Bardina, Ferziger & Reynolds (1980), which has been found to give a relatively high correlation with the actual SGS stress tensor in *a priori* tests, but does not give an extra contribution in the case of spectral cut-off filters. This method has been extended to incorporate filters at different levels in the formulation and improved to take into account the shape of the filter kernel (Geurts 1997). The use of a wider filter does, however, give a larger length scale of the model which might have an undesirable influence on the larger scales of the flow.

There are other, more recent, models that have the potential to yield good predictions for the SGS stress tensor, e.g. the velocity estimation model (Domaradzki & Saiki 1997) which is based on the definition of τ_{ij}. These are, however, at an early stage of development and their performance is therefore relatively unexplored. The effect of backscatter might be important to model and an extra stochastic term, which

acts on the smallest scales, is desirable. However, in all LES there will always be an uncertainty with regards to the effect of the SGS model.

When applying a filter to the NS equations the result typically becomes dependent on the coordinate system used to describe the filter. This is described in detail by Oberlack (1997), where it is shown that the symmetries of the original equations are generally not kept when applying a filter. In particular the equations may show a non-invariant behaviour with e.g. system rotation, depending on the type of filter and the SGS stress model, and the problem with the filter only enters when it is applied explicitly. It has also been found (Vreman, Guerts & Kuerten 1994) that the use of spectral cut-off filters yields a SGS stress tensor that is not realizable, in the sense that the trace τ_{kk} can be negative in the flow. This implies that τ_{kk} is not suitable to use in modelling, e.g. as a quantity to form a transport equation for. *A priori* tests show that e.g. Gaussian and top-hat filters yield a higher correlation for the SGS model with the SGS stresses (Liu, Meneveau & Katzl 1994). However, the spectral cut-off filter keeps the maximum amount of information, for a given resolution, in the resolved scales which reduces the importance of the model. Also, since for spectral cut-off filters $\overline{\overline{f}} = \overline{f}$, it is possible through explicit filtering of the equations to know what filter you actually have in the simulations, which then allows for correct computation of turbulence statistics.

The shape of the kinetic energy spectrum, at the smallest resolved scales, will directly depend on the choice of the SGS-model parameter. For instance, a high value of Ko (small C_s) will make the slope of $E(k)$ smaller than $k^{-5/3}$ whereas a smaller value of Ko (larger C_s) will cause the slope to become steeper than $k^{-5/3}$. This is seen in e.g. Métais & Lesieur (1992) where they used the value $Ko = 1.5$ which resulted in a k^{-2} spectrum instead of a $k^{-5/3}$, which was obtained in the simulations by Chasnov (1991, 1994) who used the larger value $Ko = 2.1$.

2.3. *The numerical simulations*

Simulations with 256^3 spectral modes have been performed using a pseudospectral method with a second-order mixed Crank–Nicolson and Adams–Bashforth time-stepping method. The computational domain size is $L_x = L_y = L_z = 2\pi\mathscr{L}$, which gives a cut-off wavenumber of $k_c = 127k_0$, where $k_0 = 1/\mathscr{L}$. A 3/2 dealiasing method is implemented in physical space where the nonlinear terms are calculated.

In the decaying turbulence simulations isotropic initial velocity fields are generated with a given energy spectrum using random phases. The initial energy spectrum was given with a k^2 low-wavenumber slope. These velocity fields are strained axisymmetrically in the x_1-direction according to rapid distortion theory with a total strain of $c = 2.25$ to yield a cubic domain and then relaxed towards isotropy. Results are taken from the simulations when a self-similar decay of the energy spectrum has been obtained.

The forced turbulence simulation starts from a zero velocity field, where the random force generates the turbulence. The forcing wavenumber is set to a low value, $k_f = 2k_0$, so that it will have little influence on the high-wavenumber dynamics. In order to generate axisymmetric turbulence states the input power in the u_2 and u_3 components is set to be 23 times larger than in the u_1 component. Statistics are gathered from the simulation when a statistically stationary state has been reached and the two-point correlations have developed.

Since the small scales are modelled in the LES the Kolmogorov microscale is unknown. This also leaves the Reynolds number as unknown. In the forced DNS of Alvelius (1999) it is seen that $k_{\text{inert}}\eta \approx 0.1$, where k_{inert} is the wavenumber at the end

of the inertial subrange. If we take $k_{\text{inert}} = k_c$ in the LES the Kolmogorov microscale can be estimated as $\eta = 0.1/k_c$. The small scale η is related to the viscosity ν through $\eta = (\nu^3/\epsilon)^{1/4}$. The turbulence Reynolds number,

$$Re_T = \frac{4K^2}{\nu\epsilon}, \tag{2.9}$$

in the forced and decaying turbulence simulations, can then be estimated to be as high as $Re_T = 330\,000$ and $Re_T = 80\,000$, respectively. From DNS (Alvelius 1999) it is seen that the compensated energy spectrum $E(k)k^{5/3}$ actually has a bump at the end of the inertial subrange ($k\eta = 0.17$) associated with a maximum in the dissipation spectrum. This implies that $E(k)k^{5/3}$ should actually increase, as it does in the LES close to k_c, before it decreases. If it is assumed that the cut-off wavenumber, k_c, is localized at the position of maximum dissipation, we get $\eta = 0.17/k_c$ (instead of $0.1/k_c$) which gives the estimates $Re_T = 160\,000$ and $Re_T = 40\,000$ for the two simulations.

In isotropic turbulence the dissipation is related to the Taylor microscale, λ, through

$$\epsilon = \frac{10\nu K}{\lambda^2}. \tag{2.10}$$

Using the velocity scale $q = (2K/3)^{1/2}$ the Taylor-microscale Reynolds number Re_λ can, in the isotropic case, be expressed as

$$Re_\lambda = \left(\tfrac{15}{9}\right)^{1/2} Re_T^{1/2}. \tag{2.11}$$

With the lower estimates of Re_T for the forced and decaying simulations the Taylor-microscale Reynolds number is estimated through (2.11) as $Re_\lambda = 516$ and $Re_\lambda = 258$.

3. Results

The kinetic energy spectrum, the pressure spectrum and the second- and third-order structure functions are computed in order to verify the existence of an inertial subrange and to identify the range of scales for which the inertial laws are valid. In particular the agreement of the simulation results with the theory of Lindborg (1996) for P_l is compared to the corresponding agreement for the theory of the second- and third-order structure functions. The degree of Reynolds stress anisotropy is measured by the anisotropy tensor $a_{ij} \equiv \langle u_i u_j \rangle / K - 2\delta_{ij}/3$. The results from the simulations are evaluated at the anisotropy value $a_{11} = -0.15$ for the decaying turbulence case and at the statistically stationary value $a_{11} = -0.2$ for the forced turbulence case. In the present section results are only presented for the spectral model with $Ko = 2.2$. In § 4 results are given for the Smagorinsky model, with $C_s = 0.1$, and the spectral model with $Ko = 1.7$, in order to investigate how sensitive the results are to the choice of SGS model.

The first and second hypotheses of similarity by Kolmogorov (1941*b*) give the following relation for the second-order structure function:

$$B_{ll} = C(\epsilon r)^{2/3}, \tag{3.1}$$

valid for inertial-subrange separations. C is a constant, independent of the flow. The spectral equivalent of this relation is the inertial subrange for the kinetic energy spectrum

$$E(k) = C_1 \epsilon^{2/3} k^{-5/3}. \tag{3.2}$$

The second-order structure function B_{ll} in figure 1 shows that an inertial subrange

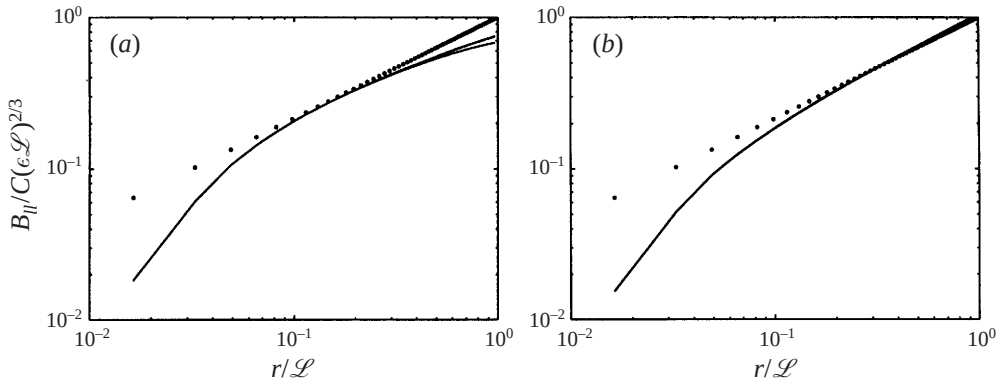

FIGURE 1. The two-point correlations $B_{ll}/(C(\epsilon\mathscr{L})^{2/3})$ for $l = 1, 2, 3$ (solid curves) and the curve $(r/\mathscr{L})^{2/3}$ for which each dot indicates a grid point in the simulations. (*a*) Decaying turbulence, $C = 1.7$. (*b*) Forced turbulence, $C = 2.1$.

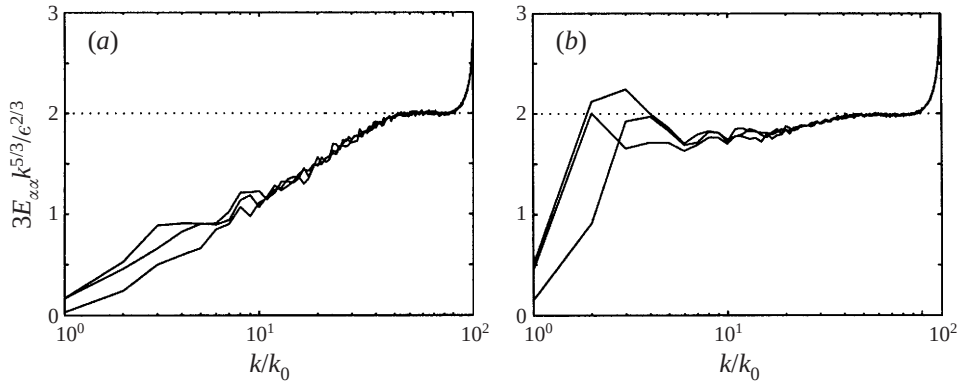

FIGURE 2. The compensated energy spectra $3E_{\alpha\alpha}k^{5/3}/\epsilon^{2/3}$, $\alpha = 1, 2, 3$. (*a*) Decaying turbulence. (*b*) Forced turbulence.

can be perceived in both simulations. The different components of B_{ll} collapse onto each other. The decaying simulation yields the value $C = 1.7$ of the Kolmogorov constant related to this structure function whereas the forced simulation gives a larger inertial subrange with the value $C = 2.1$. In a comparison with several different experiments Antonia *et al.* (1996) obtained the value $C = 2.0$ which is in good agreement with the results from the present forced simulation. For larger values of r in the decaying turbulence the longitudinal second-order structure function for $l = 1$ (the axis of symmetry) falls somewhat below the others for $l = 2,\ 3$ (which collapse).

An inertial subrange yields a constant value of $3E_{\alpha\alpha}k^{5/3}/\epsilon^{2/3}$. In figure 2 the inertial subrange appears at the high end of wavenumbers in the simulations with a cusp (typical for this type of LES) close to the cut-off wavenumber k_c. Both simulations (figure 2) give the Kolmogorov constant $C_1 = 2.0$ related to the energy spectrum. The inertial law is however valid in a slightly wider range for the forced simulation and at lower wavenumbers the deviation from the inertial law is much smaller compared to the decaying turbulence simulation.

The values of C_1 presented in the literature vary. Chasnov (1991) presents values found in experiments and simulations which vary between $C_1 = 1.34$ and 2.45. Praskovsky & Oncley (1994) found in their measurements that C_1 decreased with

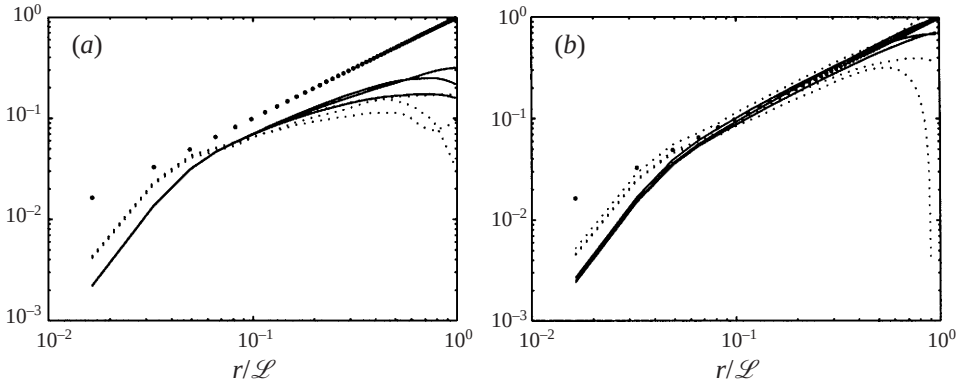

FIGURE 3. The two-point correlations $-5B_{lll}/(4\epsilon\mathscr{L})$, $l = 1, 2, 3$ (solid curves), $-15B_{ltt}/(4\epsilon\mathscr{L})$ (small dotted curves) and the curve $r/\mathscr{L}$ (large dots). (*a*) Decaying turbulence. (*b*) Forced turbulence.

increasing Reynolds number. There is a theoretical relation, at infinite Reynolds number, between the two Kolmogorov constants $C_1 = 0.76C$ (Monin & Yaglom 1975). The finite Reynolds number in the present simulations gives $C_1/C = 1.18$ from the decaying simulation and $C_1/C = 0.95$ from the forced simulation. Van Atta & Chen (1970) obtained the ratio $C_1/C = 0.92$, where they attributed the difference with theory to the spectral contribution outside the inertial subrange.

The tensor B_{ijk} B_{ijk} is completely determined by the two components B_{lll} and B_{ltt}. These are related through the incompressibility condition (Monin & Yaglom 1975)

$$B_{ltt} = \frac{1}{6}\frac{\mathrm{d}}{\mathrm{d}r}(rB_{lll}), \tag{3.3}$$

which together with the four-fifths law in the inertial range

$$B_{lll} = -\tfrac{4}{5}\epsilon r \tag{3.4}$$

gives that

$$B_{ltt} = -\tfrac{4}{15}\epsilon r. \tag{3.5}$$

The functional form of the theoretical inertial-range relations can simply be derived from dimensional analysis. The difference between the relations (3.4), (3.5) and (1.4) compared to (3.1) and (3.2) is that the unknown constants are obtained from the Navier–Stokes equations.

Figure 3 shows the third-order structure functions B_{lll} and B_{ltt}. In the forced simulation there is a good agreement between the results and theory while in the decaying simulation the theory is only seen to be approximately satisfied. In the forced case both B_{lll} and B_{ltt} adhere closely to the expected line over a span of separations that cover about a decade.

It is apparent that the second-order structure function follows its theoretical behaviour longer than the third-order structure functions. This can be attributed to the fact that only the derivatives of B_{ll} have to be zero at the separation $r/\mathscr{L} = \pi$ (half the box length), while the functions B_{lll} and B_{ltt} themselves have to be zero at the same separation. However, this behaviour is also seen in experimental measurements which suggests that the reason could be dynamic. The real inertial subrange should here be seen as the region where the third-order structure functions follow their well known theoretical behaviour.

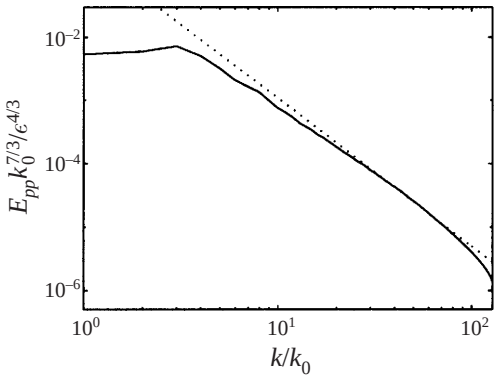

FIGURE 4. The pressure spectrum $E_{pp}k_0^{7/3}/\epsilon^{4/3}$ (solid curve) and the (dotted) line $C_p(k/k_0)^{-7/3}$ with $C_p = 5.0$.

Batchelor (1953) showed that the two-point pressure correlation $\langle(\delta p)^2\rangle/\rho^2$ should be equal to $(B_{ll})^2 \sim r^{4/3}$ in the inertial subrange. This readily gives that the pressure spectrum, E_{pp}, in the inertial subrange should be of the form

$$E_{pp} = C_p \epsilon^{4/3} k^{-7/3}, \tag{3.6}$$

where C_p is a universal constant. George, Beuther & Arndt (1984) verified this behaviour in the mixing layer of an axisymmetric jet. Elliot (1972) and Albertson *et al.* (1998) obtained lower values of the exponent. From the forced simulation a small region with a $k^{-7/3}$ slope is perceived (figure 4) for E_{pp} with $C_p = 5.0$ in the inertial subrange. Close to k_c the pressure spectrum falls below the inertial-range law as opposed to the kinetic energy spectrum.

The simulations are globally homogeneous and locally isotropic. In a globally homogeneous case it directly follows from the condition $T_{ij} = 0$ that

$$\frac{\partial P_i}{\partial r_j} + \frac{\partial P_j}{\partial r_i} = -2\Pi_{ij}, \tag{3.7}$$

where the pressure–strain rate tensor Π_{ij} is non-zero for globally anisotropic cases such as the present. Putting both free indices equal to l gives

$$\frac{\partial P_l}{\partial r_l} = -\Pi_{ll}, \tag{3.8}$$

and the relation (1.4) is simply recovered by integration of (3.8).

In the decaying simulation (figure 5*a*) the low Reynolds number prevents conclusive validation of the theory. From figure 5(*b*), on the other hand, we see that the pressure–velocity correlation, P_l, follows its theoretical linear behaviour for separations well into the inertial subrange for the forced simulation. Hence, P_l is clearly seen to be non-zero and, in accordance with the theory of Lindborg (1996), of the same order of magnitude as the third-order structure functions and the pressure–strain term towards the end of the inertial subrange.

The pressure term T_{ij} is much smaller than ϵ (figure 6) for the same range of separations r where P_l adheres to the theoretical linear behaviour. Figures 5 and 6 give a numerical verification of the theories of Lindborg (1996) and Hill (1997).

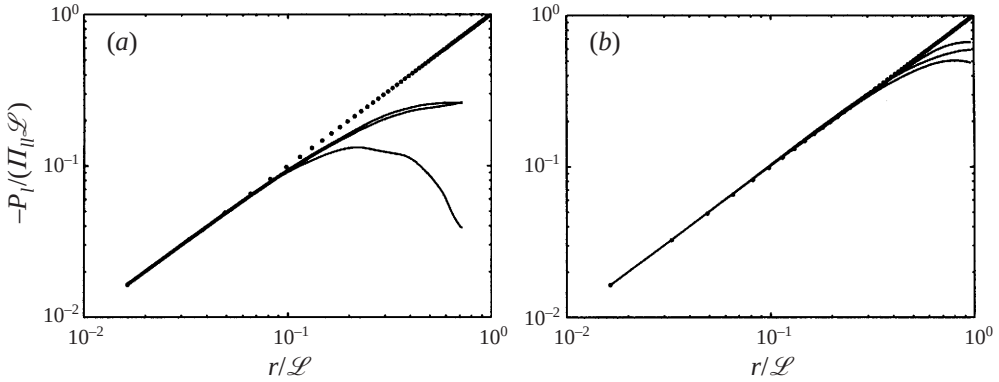

FIGURE 5. The two-point correlations $-P_l/\Pi_{ll}\mathscr{L}$, $l = 1, 2, 3$ (solid curves) and the line $r/\mathscr{L}$ (dots). (*a*) Decaying turbulence. (*b*) Forced turbulence.

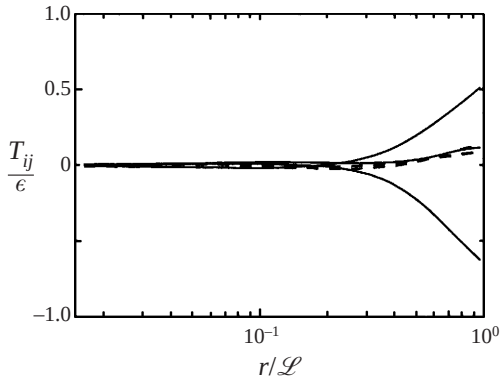

FIGURE 6. The tensor components $T_{ij}(r)/\epsilon$, averaged over all directions of $\boldsymbol{r}$, for the forced simulations. Solid curves: the diagonal ($i = j$) components, dashed curves: off-diagonal ($i \neq j$) components.

4. Sensitivity to choice of SGS stress model

Since the effect of the SGS stress model on the results is unknown it is important to investigate how sensitive the results are to its choice. This is done by also performing the forced simulations with the Smagorinsky model, and with another choice of Ko for the spectral model.

The Smagorinsky constant was set to $C_s = 0.1$, which yields an inertial subrange for the kinetic energy spectrum (figure 7*a*) with a Kolmogorov constant $C_1 = 1.7$. The second-order structure function B_{ll} shows the same behaviour as for the spectral model (with $Ko = 2.2$), with the Kolmogorov constant $C = 2.0$. This gives the ratio $C_1/C = 0.85$, which is actually closer to the theoretical value (0.76). The third-order structure functions agree well with theory (figure 7*b*) and it is verified that an inertial subrange exists also in these simulations. The two-point pressure–velocity correlation shows a good adherence to the theoretical linear behaviour (figure 8*a*) in the inertial subrange. The pressure spectrum also gives the same behaviour as the spectral model, with the constant $C_p = 5.0$.

As is seen in the simulations by Chasnov (1991) and Métais & Leisieur (1992) the shape of the kinetic energy spectrum is strongly influenced by the SGS model parameters. The spectral model with $Ko = 1.7$ indeed yields a kinetic energy spectrum

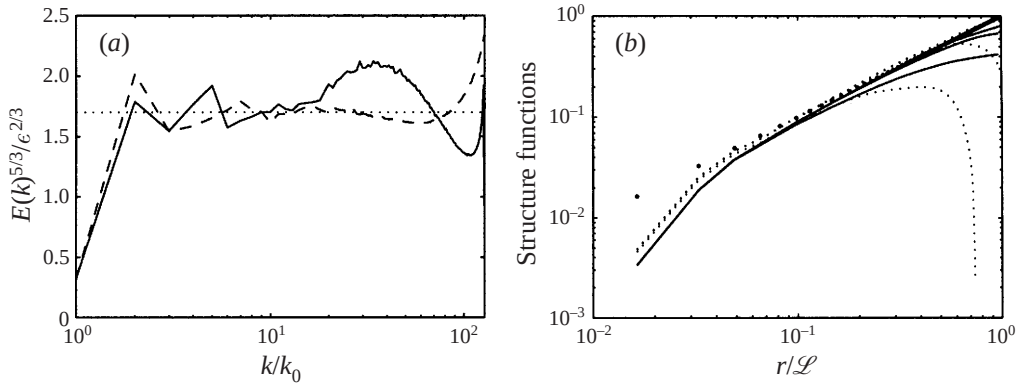

FIGURE 7. (*a*) The compensated kinetic energy spectrum $E(k)k^{5/3}/\epsilon^{2/3}$ for the Smagorinsky model (dashed curve) and the spectral model with $Ko = 1.7$ (solid curve) together with the constant value 1.7 (dotted line). (*b*) The two-point correlations (using the Smagorinsky model) $-5B_{lll}/(4\epsilon\mathscr{L})$, $l = 1, 2, 3$ (solid curves), $-15B_{ltt}/(4\epsilon\mathscr{L})$ (small dotted curves) and the curve $r/\mathscr{L}$ (large dots).

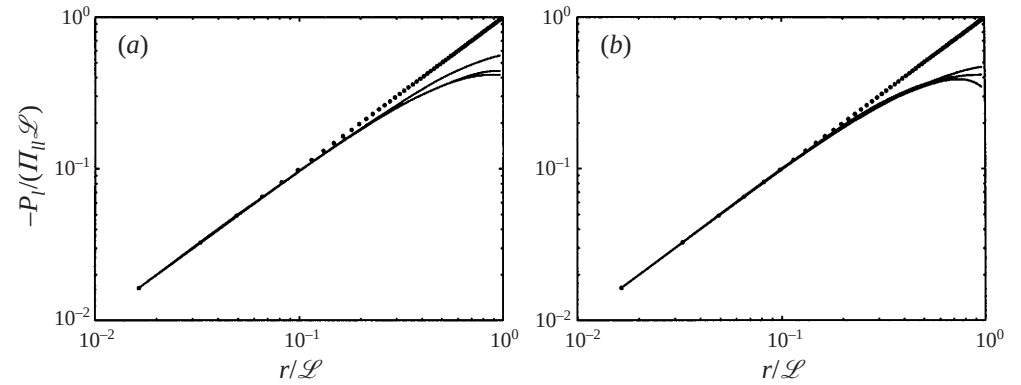

FIGURE 8. The two-point correlations $-P_l/\Pi_{ll}\mathscr{L}$, $l = 1, 2, 3$ (solid curves) and the line $r/\mathscr{L}$ (dots). (*a*) With the Smagorinsky model. (*b*) With the spectral model ($Ko = 1.7$).

(figure 7*a*) with a shape different from the simulation with $Ko = 2.2$. There is no clear region with a $k^{-5/3}$ slope, and the compensated kinetic energy spectrum suggests a Kolmogorov constant in the range $C_1 \approx 1.6$–2.0 for this case. The second- and third-order structure functions, however, still agree well with theory (with $C = 2.0$), and the pressure–velocity correlation adheres closely to the theoretical linear behaviour (figure 8*b*). The pressure spectrum is, however, slightly changed to yield a constant $C_p = 6.0$.

5. Conclusions

The forced simulation gives an inertial subrange which is in good agreement with the Kolmogorov theories for the energy spectrum and the second- and third-order structure functions. These simulations also give a pressure–velocity correlation which agrees well with the new theory of Lindborg (1996) and verifies the vanishing of T_{ij} in the inertial subrange (Hill 1997). In the decaying simulation the Reynolds number is too low to allow a conclusive validation of the theory. The forcing methodology, hence, is here essential in extending the range of problems for which the simulation

tool can fruitfully be used to study turbulence dynamics. The results from the LES are validated also by use of different SGS stress models and different model parameters. Even though the kinetic energy spectrum shows a relatively strong dependence on the model, the results for the two-point correlations are more or less insensitive.

The new extensions (Lindborg 1996 and Hill 1997) of the Kolmogorov theory are hence, for the first time verified from (numerical) experiments. The results show, as expected from the theory, that when the turbulence is globally anisotropic then the pressure–velocity correlation in fact varies linearly in a major part of the inertial subrange. The pressure term T_{ij} is also shown to be small in the inertial range which is in agreement with the theory of Hill (1997) and with the linear behaviour of P_l. The behaviour of B_{lll} and B_{ltt} also verifies that the Kolmogorov equation is correct under the assumption of local isotropy even when there is significant anisotropy in the energy distribution on the large scales. This is actually the first numerical verification of the Kolmogorov equations in globally anisotropic turbulence.

The authors wish to thank Dr Erik Lindborg for fruitful discussions on the present topic.

REFERENCES

Albertson, J. D., Katul, G. G., Parlange, M. B. & Eichinger, W. E. 1998 Spectral scaling of static pressure fluctuations in the atmospheric surface layer: The interaction between large and small scales. *Phys. Fluids* **10**, 1725–1732.

Alvelius, K. 1999 Random forcing of three-dimensional homogeneous turbulence. *Phys. Fluids* A **11**, 1880–1889.

Alvelius, K., Hallbäck, M. & Johansson, A. V. 1999 An LES study of the self consistency of the Smagorinsky model and calibration of slow-pressure strain rate models. *Eur. J. Mech.* B/*Fluids* Submitted for publication.

Antonia, R. A., Zhu, T., Anselmet, F. & Ould-Ruis, M. 1996 Comparison between the sum of second-order velocity structure functions and the second-order temperature structure function. *Phys. Fluids* A **8**, 3105–3111.

Bardina, J., Ferziger, J. H. & Reynolds, W. C. 1980 Improved subgrid scale models for large eddy simulation. *Paper* 80-0825.

Batchelor, G. K. 1953 *The Theory of Homogeneous Turbulence*. Cambridge University Press.

Chasnov, J. R. 1991 Simulation of the Kolmogorov inertial subrange using an improved subgrid model. *Phys. Fluids* A **3**, 188–200.

Chasnov, J. R. 1994 Similarity states of passive scalar transport in isotropic turbulence. *Phys. Fluids* **6**, 1036–1051.

Chollet, J. P. 1984 Two-point closure used for a sub-grid scale model in large eddy simulations. In *Turbulent Shears Flow IV* (ed. F. Durst & B. Launder), pp. 62–72. Springer.

Deardorff, J. W. 1970 A numerical study of three-dimensional turbulent channel flow at large Reynolds numbers. *J. Fluid Mech.* **41**, 453–480.

Domaradzki, J. A. & Saiki, E. M. 1997 A subgrid-scale model based on the estimation of unresolved scales of turbulence. *Phys. Fluids* **9**, 2148–2164.

Elliot, J. A. 1972 Microscale pressure fluctuations measured within the lower atmospheric boundary layer. *J. Fluid Mech.* **53**, 351–383.

Frisch, U. 1995 *Turbulence*. Cambridge University Press.

George, W. K., Beuther, P. D. & Arndt, R. E. A. 1984 Pressure spectra in turbulent free shear flows. *J. Fluid Mech.* **148**, 155–191.

Germano, M., Piomelli, U., Moin, P. & Cabot, W. H. 1991 A dynamic subgrid-scale eddy viscosity model. *Phys. Fluids* **3**, 1760–1765.

Geurts, B. J. 1997 Inverse modeling for large-eddy simulation. *Phys. Fluids* **9**, 3585–3587.

Hill, R. J. 1997 Applicability of Kolmogorov's and Monins's equations of turbulence. *J. Fluid Mech.* **353**, 67–81.

KOLMOGOROV, A. N. 1941*a* Dissipation of energy in the locally isotropic turbulence. *C. R. Acad. Sci. URSS* **32**, 16 (reprinted in *Proc. R. Soc. Lond.* A **434** (1991), 15–17).

KOLMOGOROV, A. N. 1941*b* The local structure of turbulence in incompressible viscous fluid for very large Reynolds numbers. *C. R. Acad. Sci. URSS* **30**, 301 (reprinted in *Proc. R. Soc. Lond.* A **434** (1991), 9–13).

LINDBORG, E. 1996 A note on Kolmogorov's third order structure function law, the local isotropy hypothesis and the pressure-velocity correlation. *J. Fluid Mech.* **326**, 343–356.

LINDBORG, E. 1999*a* Correction to the four-fifths law due to variations of the dissipation. *Phys. Fluids* **11**, 510–512.

LINDBORG, E. 1999*b* The pressure terms in the general Kolmogorov equation. *Phys. Fluids* Submitted for publication.

LIU, S., MENEVEAU, C. & KATZ, J. 1994 Experimental study of similarity subgrid-scale models of turbulence in the far-field of a jet. In *Direct and Large-Eddy Simulation I* (ed. P. R. Voke, L. Kleiser & J.-P. Chollet.), pp. 37–48. Kluwer.

MÉTAIS, O. & LESIEUR, M. 1992 Spectral large-eddy simulation of isotropic and stably stratified turbulence. *J. Fluid Mech.* **239**, 157–195.

MONIN, A. S. & YAGLOM, A. M. 1975 *Statistical Fluid Mechanics: Mechanics of Turbulence*, vol. 2. The MIT Press.

OBERLACK, M. 1997 Invariant modelling in large-eddy simulation of turbulence. *Center for Turbulence Research, Stanford University, Annual Research Briefs,* pp. 3–22.

PIOMELLI, U. 1994 High Reynolds number calculations using the dynamic subgrid-scale stress model. *Phys. Fluids* A **5**, 1484–1490.

PRASKOVSKY, A. & ONCLEY, S. 1994 Measurements of the Kolmogorov constant and intermittency exponent at very high Reynolds numbers. *Phys. Fluids* A **6**, 2886–2888.

SMAGORINSKY, J. 1963 General circulation experiments with the primitive equations. *Mon. Weath. Rev.* **91**, 99–164.

VAN ATTA, C. W. & CHEN, W. Y. 1970 Structure functions of turbulence in the atmospheric boundary layer over the ocean. *J. Fluid Mech.* **44**, 145–159.

VREMAN, B., GEURTS, B. & KUERTEN, H. 1994 Realizability conditions for the turbulent stress tensor in large-eddy simulation. *J. Fluid Mech.* **278**, 351–362.

YAGLOM, A. M. 1998 New remarks about old ideas of Kolmogorov. In *Advances in Turbulence VII* (ed. U. Frisch), pp. 605–610. Kluwer.